



TAO detector as a unique antineutrino spectrometer for fundamental and applied research

On behalf of JUNO collaboration
Alexander Chepurnov
*Lomonosov Moscow State University,
Skobelcyn Institute for Nuclear Physics*



Jul 1 – 6, 2025 St. Petersburg State University

Participation in the Conference was supported by State project “Science” by the Ministry of Science and Higher Education of the Russian Federation under the contract 075- 15-2024-541

Nuclear power reactors are the most powerful controlled artificial anti-matter generators



АЭС «Тайшань» © TNPJVC

Applied antineutrino physics

Non-proliferation of fissile materials

Monitoring (measurement) of reactor thermal power

Investigation of burnup processes for new types of nuclear fuel and new types of nuclear reactors

$\bar{\nu}_e$

- spectrum
- isotopic yields
- flux

- Initial nuclear fuel composition
- Nuclear database
- Electron spectrum for thermal neutron fission of main U/Pu isotopes

Fundamental physics

Measuring of neutrino oscillation parameters

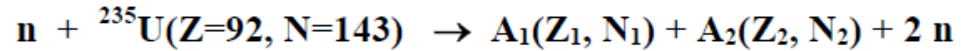
Light sterile neutrinos search

Measuring of the magnetic moment of an electron antineutrino

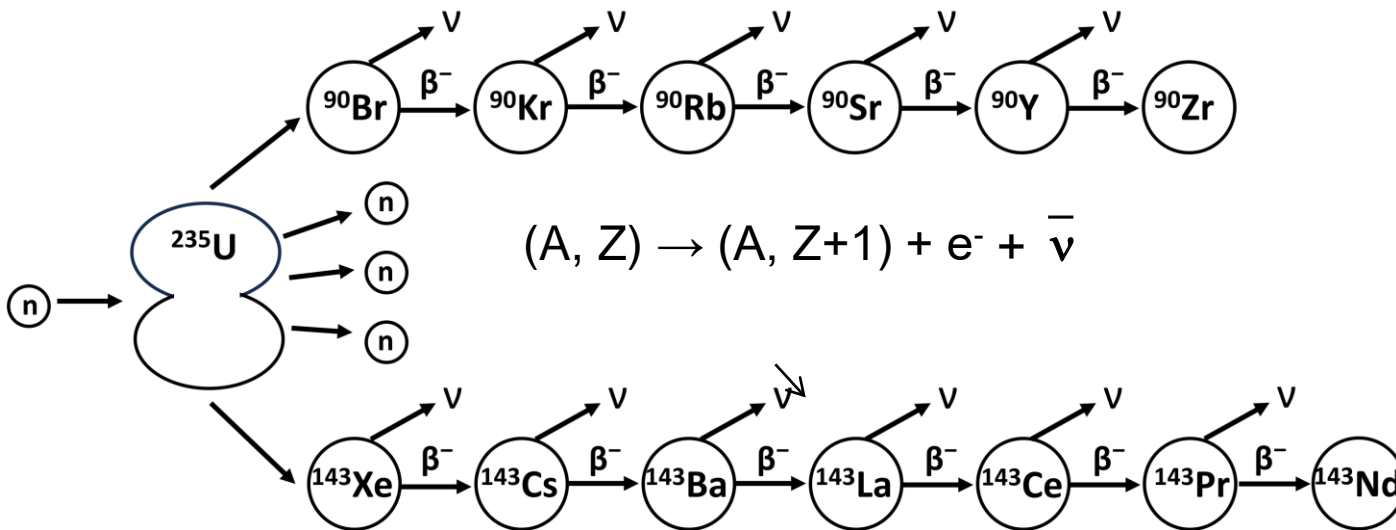
Coherent scattering of neutrinos on nuclei

Nuclear reactor as a source of reactor e⁻-antineutrinos

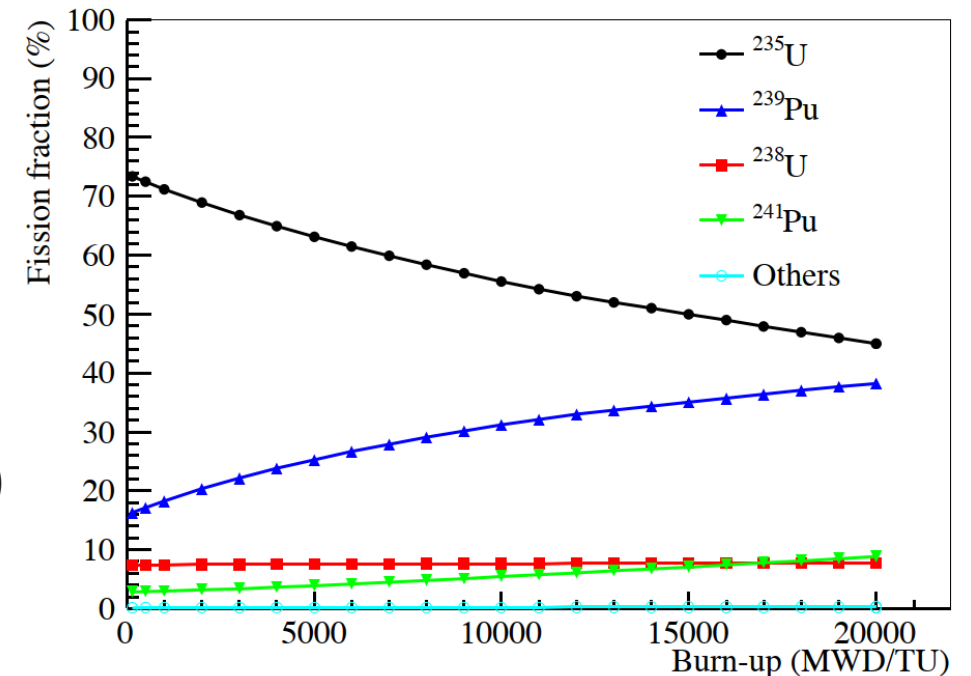
Fission isotopes have different fission product distributions.



Unstable fission products are a source of antineutrinos.
Reactors produce electron antineutrinos via the β^- -decay of neutron rich fission daughter products



arXiv:1607.05378, doi:10.1088/1674-1137/41/1/013002.



arXiv:1607.05378, doi:10.1088/1674-1137/41/1/013002.

The density of the antineutrino flux, measured remotely during the operation of the reactor, is directly proportional to the number of fissions, i.e. nuclear fuel burnup rate or nuclear reactor thermal power

BUT the neutrino flux and spectrum differs between isotopes

Summary of detection channels for reactor antineutrinos.



Channel	Name	Cross Section (10^{-44} cm^2)	Threshold (MeV)
$\bar{\nu}_e + p \rightarrow e^+ + n$	inverse beta decay (IBD)	63 (59)	1.8
$\bar{\nu}_e + e^- \rightarrow \bar{\nu}_e + e^-$	ν -electron elastic scattering (ν ES)	$0.4 \cdot Z$	—
$\bar{\nu}_e + A \rightarrow \bar{\nu}_e + A$	coherent elastic ν -nucleus scattering (CE ν NS)	$9.2 \cdot N^2$	—
$\bar{\nu}_e + d \rightarrow n + n + e^+$	ν -deuteron charged current (CC) scattering	1.1	4.0
$\bar{\nu}_e + d \rightarrow n + p + \bar{\nu}_e$	ν -deuteron neutral current (NC) scattering	3.1	2.2

<https://arxiv.org/pdf/2310.13070>

The cross section is integrated over the reactor antineutrino energy distribution assuming the typical fission fractions from the four main isotopes.

For the ν ES and the CE ν NS reaction, Z and N are the total number of protons and neutrons in the target nucleus, respectively.

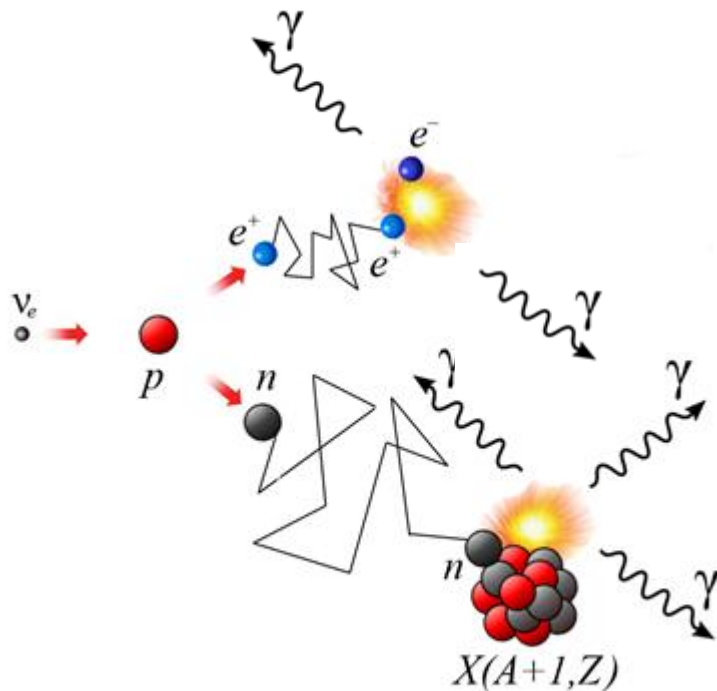
Inverse beta decay (IBD) is a magic reaction to catch reactor antineutrino

$$\bar{\nu}_e + p \rightarrow e^+ + n$$

$$dN_{e^+}(E_{e^+})/dE_{e^+} = dN_{\nu}(E_{\nu})/dE_{\nu} \times N_p \times (4\pi L^2)^{-1} \times \sigma(E_{\nu}) \times \delta_{\text{REC}}$$

$\sigma \sim 10^{-43} \text{ cm}^2$
very small !!

$$E_{e^+} = E_{\nu} - (M_n - M_p) - m_e = E_{\nu} - 1.804 \text{ MeV}$$



1 – «Prompt event» – annihilation $e^+ + e^- \rightarrow 2\gamma$
Visible energy under the condition of neglecting the recoil of the neutron $E_{\text{pt}} = E_{\nu_e} + Q + 2m_e$

2 – «Delayed event» – neutron capture followed by γ - emission $n + (A, Z) \rightarrow (A+1, Z) + \gamma$

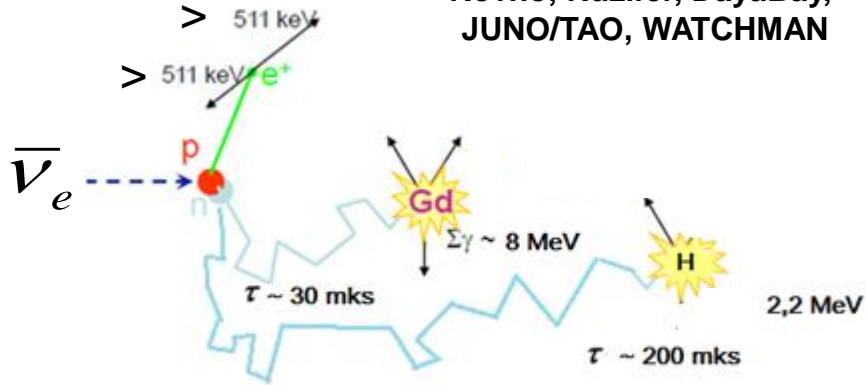
Organic liquid/plastic scintillators - most popular target material for IBD detection

- high H (p) concentration
- possible doping by Cd/Gd/ $^6\text{Li}/^{10}\text{B}$
- well developed technology

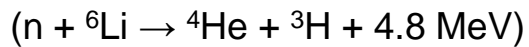
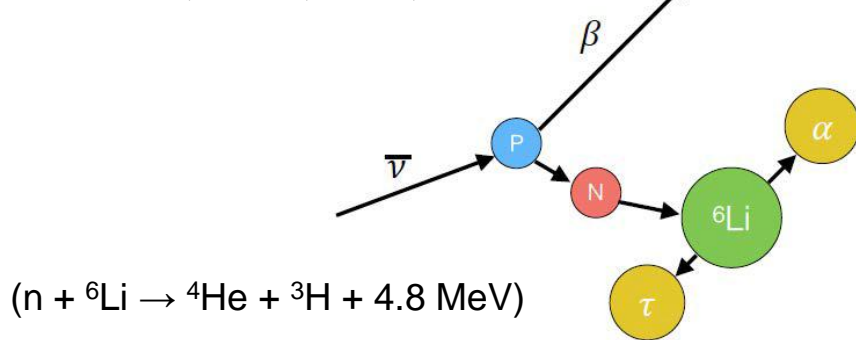
Inverse beta decay (IBD) is a magic reaction to catch reactor antineutrino

IBD "Delayed Event" registration options

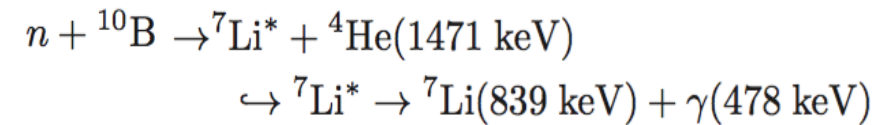
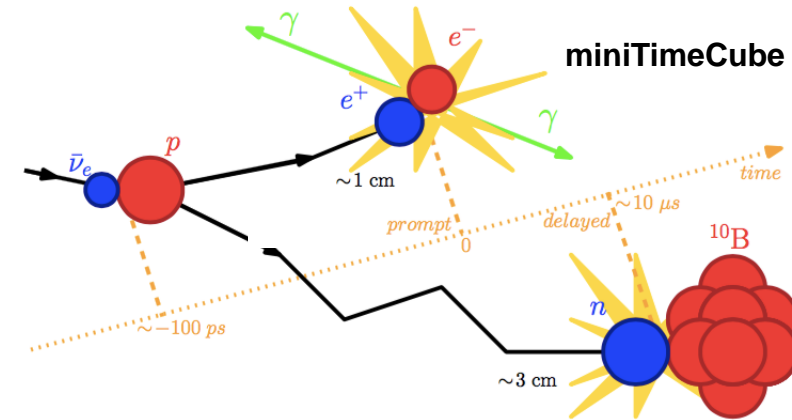
RENO, NEOS, Neutrino-4, STEREO,
PANDA, DANSS, iDREAM
Rovno, Nuzifer, DayaBay,
JUNO/TAO, WATCHMAN



PROSPECT, NuLat, SoLid, CHANDLER

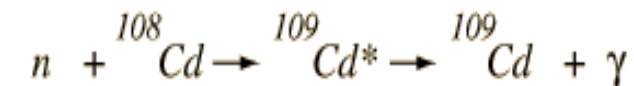


Karsten Heeger, AAP2015,



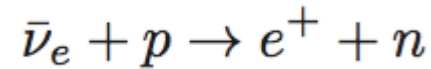
K. Nishimura - mTC @ AAP2015

What was the "very first" option??



The detection methodology of reactor neutrinos has remained unchanged over the past ~70 years.

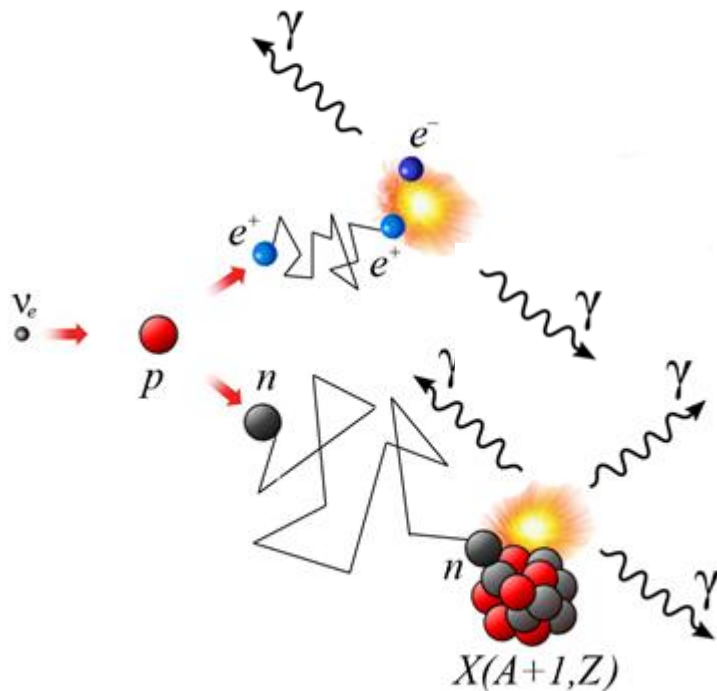
Inverse beta decay (IBD) is a magic reaction to catch reactor antineutrino



$$dN_{e^+}(E_{e^+})/dE_{e^+} = dN_{\nu}(E_{\nu})/dE_{\nu} \times N_p \times (4\pi L^2)^{-1} \times \sigma(E_{\nu}) \times \delta_{\text{REC}}$$

$\sigma \sim 10^{-43} \text{ cm}^2$
very small !!

$$E_{e^+} = E_{\nu} - (M_n - M_p) - m_e = E_{\nu} - 1.804 \text{ MeV}$$

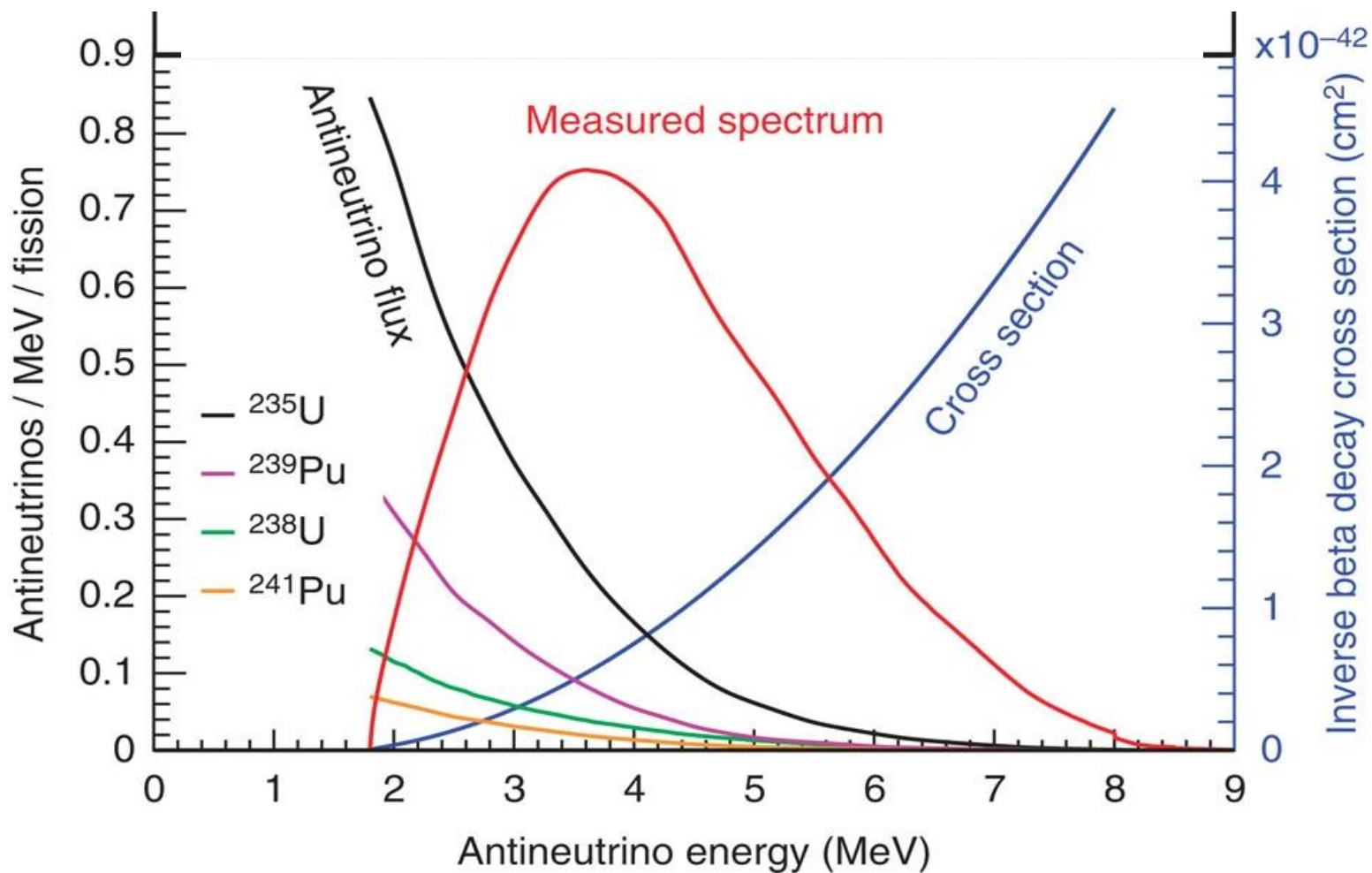


Design Optimization Goals:

TAO efforts:

- high light yield (LS properties)
- good light collection (general construction)
- minimize gamma leakages (general construction and data processing)
- effective and fast neutron capture (LS properties)
- minimize external γ/n background mimic IBD signature
 - passive shielding
 - active muon veto
 - precise time/spatial event reconstruction
- development of optimal comprehensive electronics together with sophisticated software for direct data digitizing, timing, preprocessing, storage and analysis

Reactor antineutrino detection using the inverse beta decay (IBD) reaction



Nuclear reactor monitoring with neutrino



Reactor Neutrino Detectors for flux and spectrum measurements:

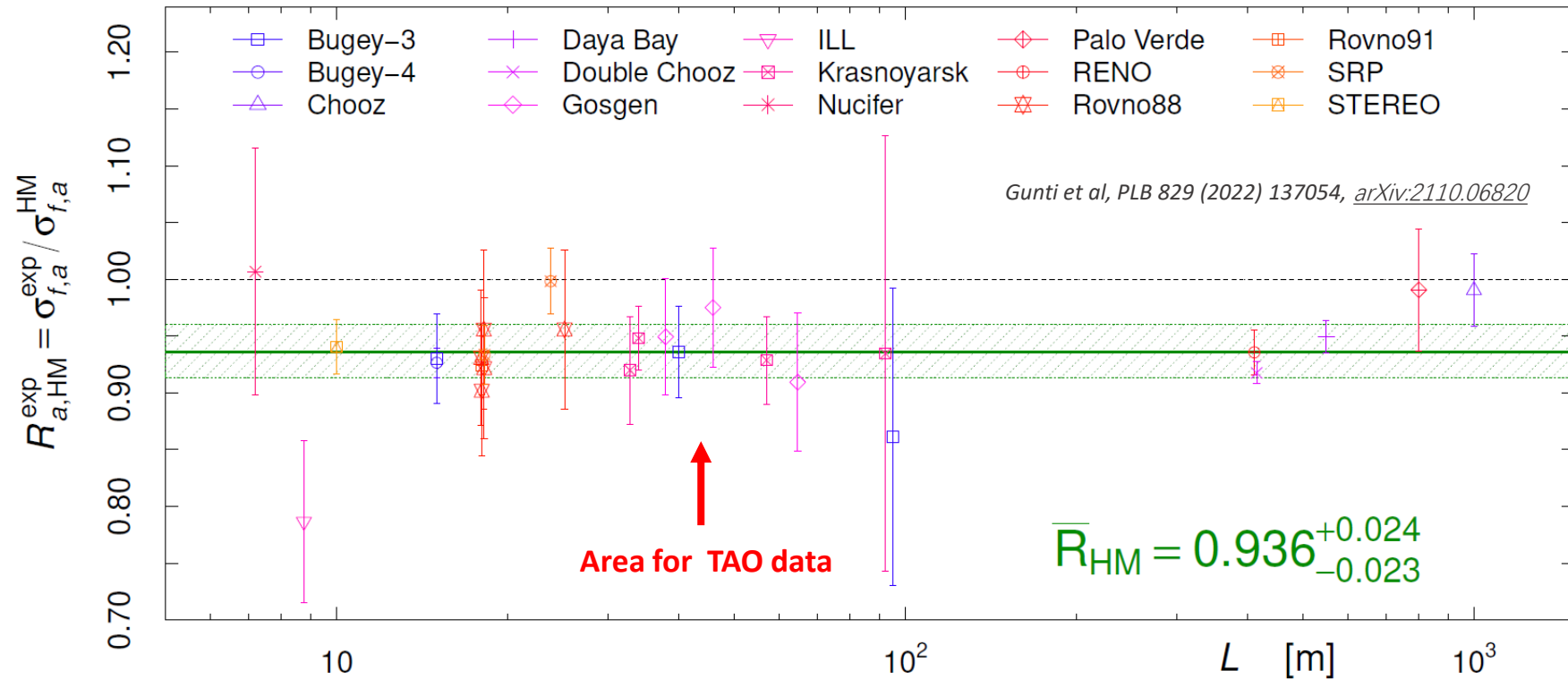
Precision Instruments with percent-level control of detection efficiencies

Energy-scale and response well understood

Θ_{13} - DayaBay, DoubleChooz, RENO, **JUNO/TAO**

Total neutrino yield measurements have achieved great precision

SBL – NEOS (-II), STEREO, PROSPECT, Neutrino-IV, DANSS, iDREAM, **TAO**



Ratio of measured and expected IBD yields for the reactor experiments as a function of the reactor-detector distance L .

The error bars show the experimental uncertainties.

Taishan Antineutrino Observatory (TAO)

Taishan **A**ntineutrino **O**bservatory (**TAO**) is a satellite experiment of **JUNO**

JUNO/TAO main goals:

- **Providing the reference model-independent spectrum for JUNO to reach the main goal - identify neutrino mass ordering (NMO)**

<https://arxiv.org/abs/2405.18008>

- **Verification of the detector technology for reactor monitoring and safeguard applications**

<https://arxiv.org/abs/2005.08745>

<https://arxiv.org/abs/2405.18008>

Other physics potential:

- **Radiative corrections in elastic neutrino-electron scattering.**

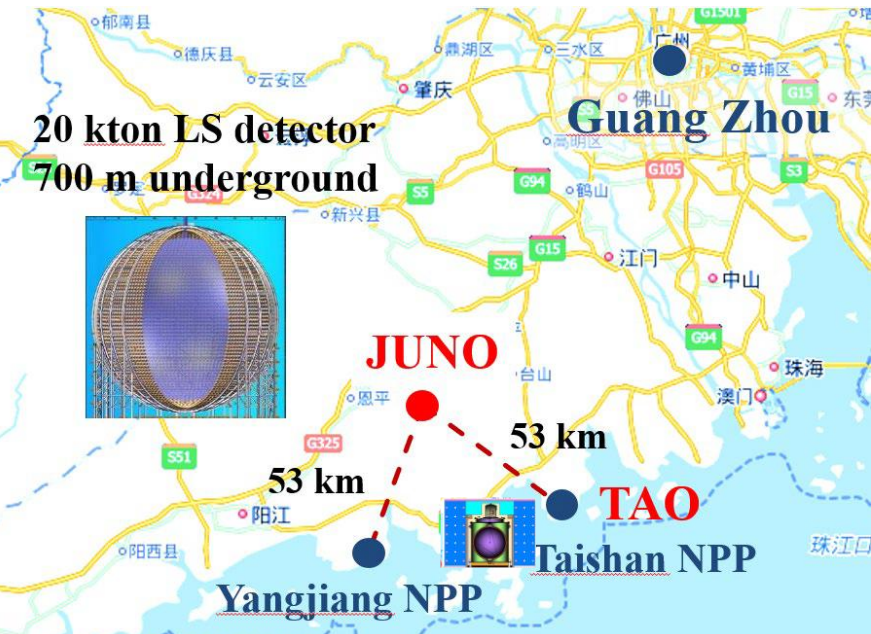
<https://arxiv.org/abs/2410.00107>

- **Light dark matter.**

<https://arxiv.org/abs/2109.04276>

Specification:

- **Expected energy resolution** - $< 2\%$ @ 1 MeV
- **Nuclear Reactor:**
 - Reactor Thermal Power - 4.59 GW
 - Reactor type – EPR
 - Baseline - 44 m (Unit 1) + 217 m (Unit 2)
- **Detector operational temperature** - -50°C
- **Target**
 - spherical acrylic vessel diameter 1.8 m (2,8 t)
 - spherical FV with radius 0.65 m (1 t)
- **Photosensors - SiPM**
 - number of tiles ~ 4024
 - 50x50x3 mm 32 SiPMs per 1 tile
 - photon detection efficiency $> 50\%$
 - coverage $\sim 94\%$
 - dark current rate $< 100 [\text{Hz}/\text{mm}^2]$
- **Scintillator**
 - LAB- based Gd-dopped
 - Light yield 12000 photons/MeV

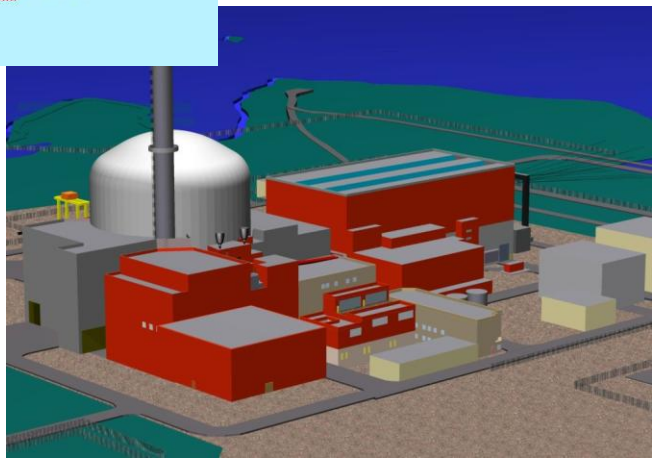


TAO detector location

The Taishan **Nuclear Power Plant** (台山核电站) features twins **EPR** Taishan 4.6 GWth reactors .
Taishan 1 started commercial operation in December 2018. It was the first NPP with operational EPR unit.
Taishan 2 started commercial operation in September 2019

The **EPR** is a third generation pressurized water reactor design. It has been designed and developed mainly by Framatome (part of Areva between 2001 and 2017) and Électricité de France (EDF) in France, and by Siemens in Germany.

In Europe this reactor design was called European Pressurized Reactor, and the internationalized name was Evolutionary Power Reactor, but is now simply named EPR



1. Reactor Building
2. Fuel Building
3. The Safeguard Buildings
4. Diesel Building
5. Nuclear Auxiliary Building
6. Waste Building

TAO is located in a basement at a baseline of 44 m from the reactor core of one of the twins EPR

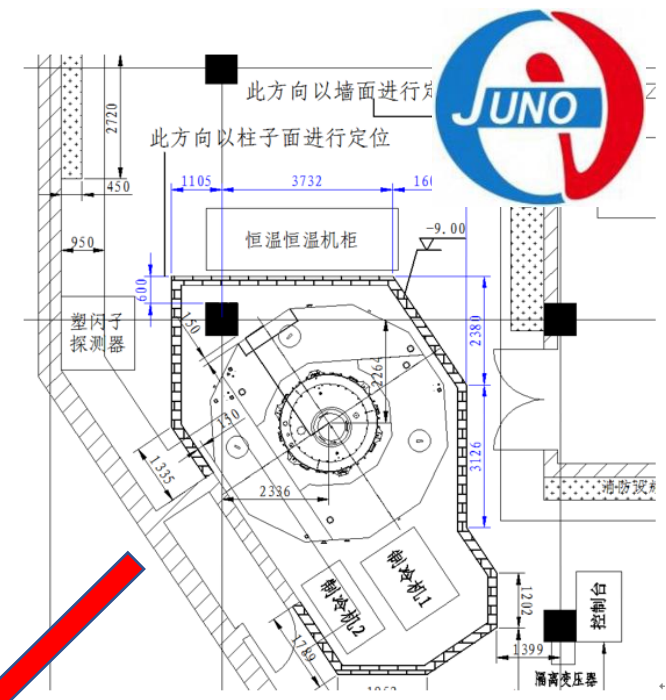
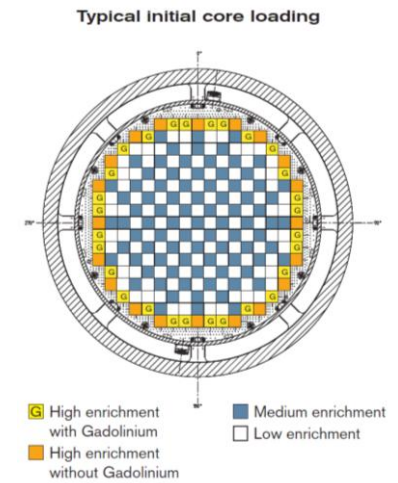
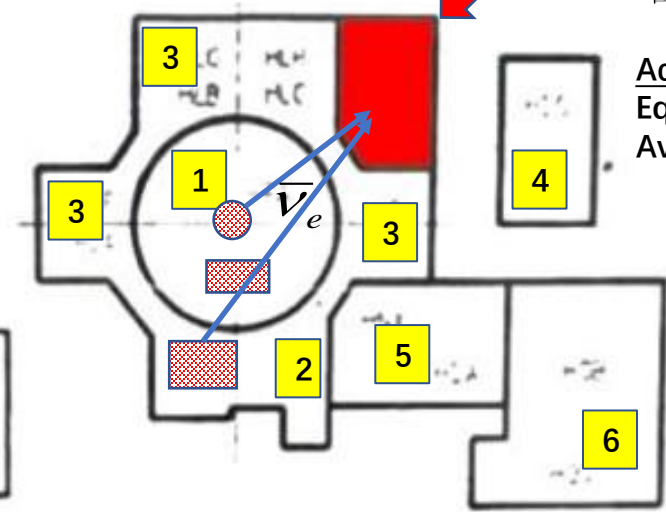


图 5.4-1 TAO 实验室消防围堰示意图

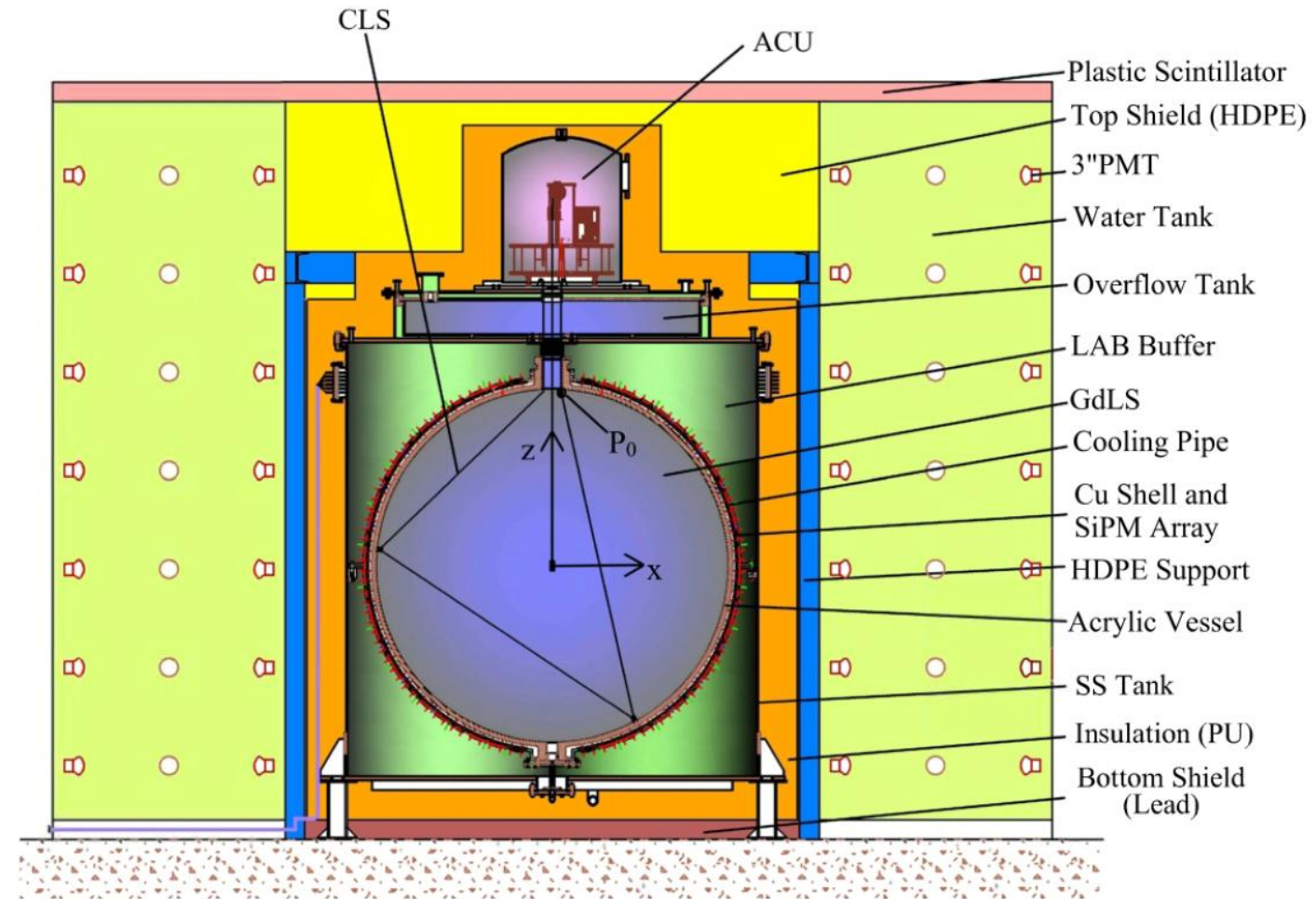
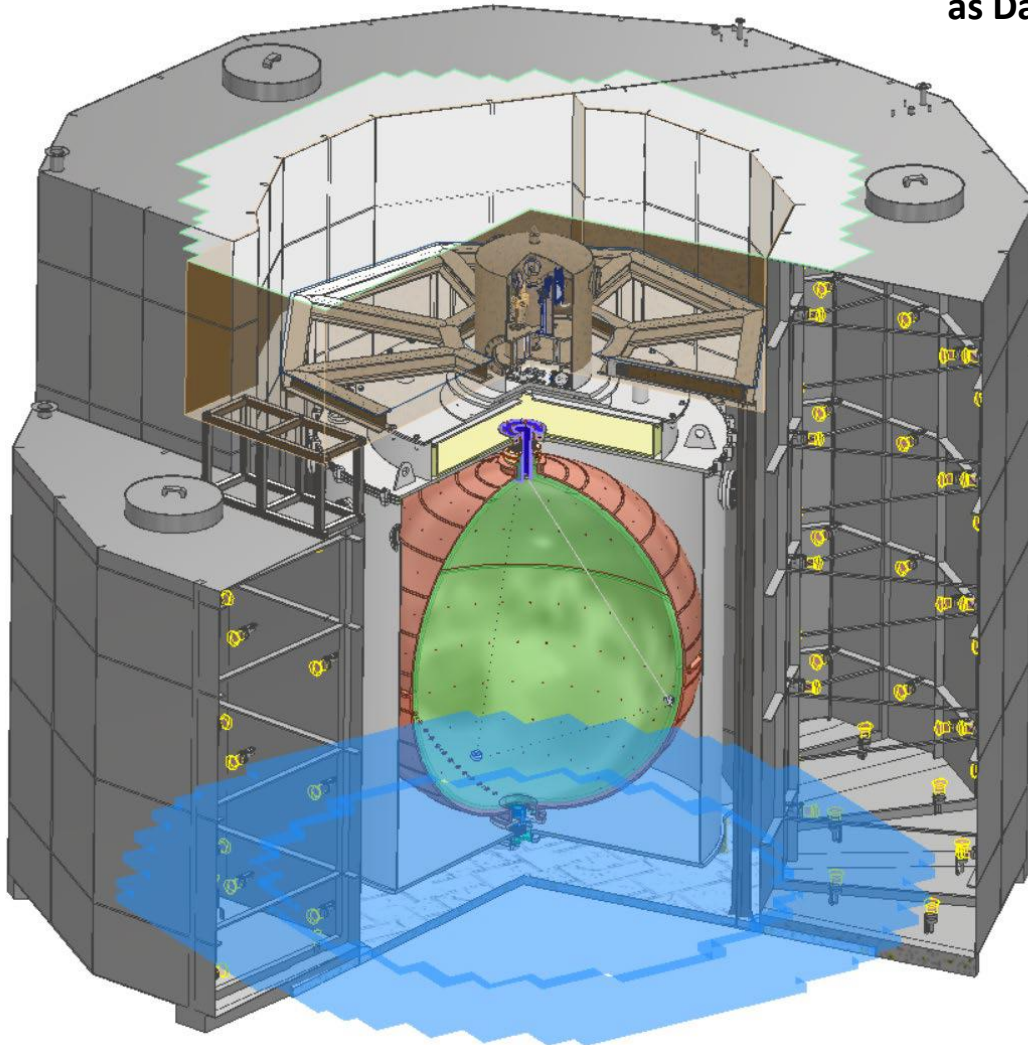


核电核岛平面图

TAO detector construction

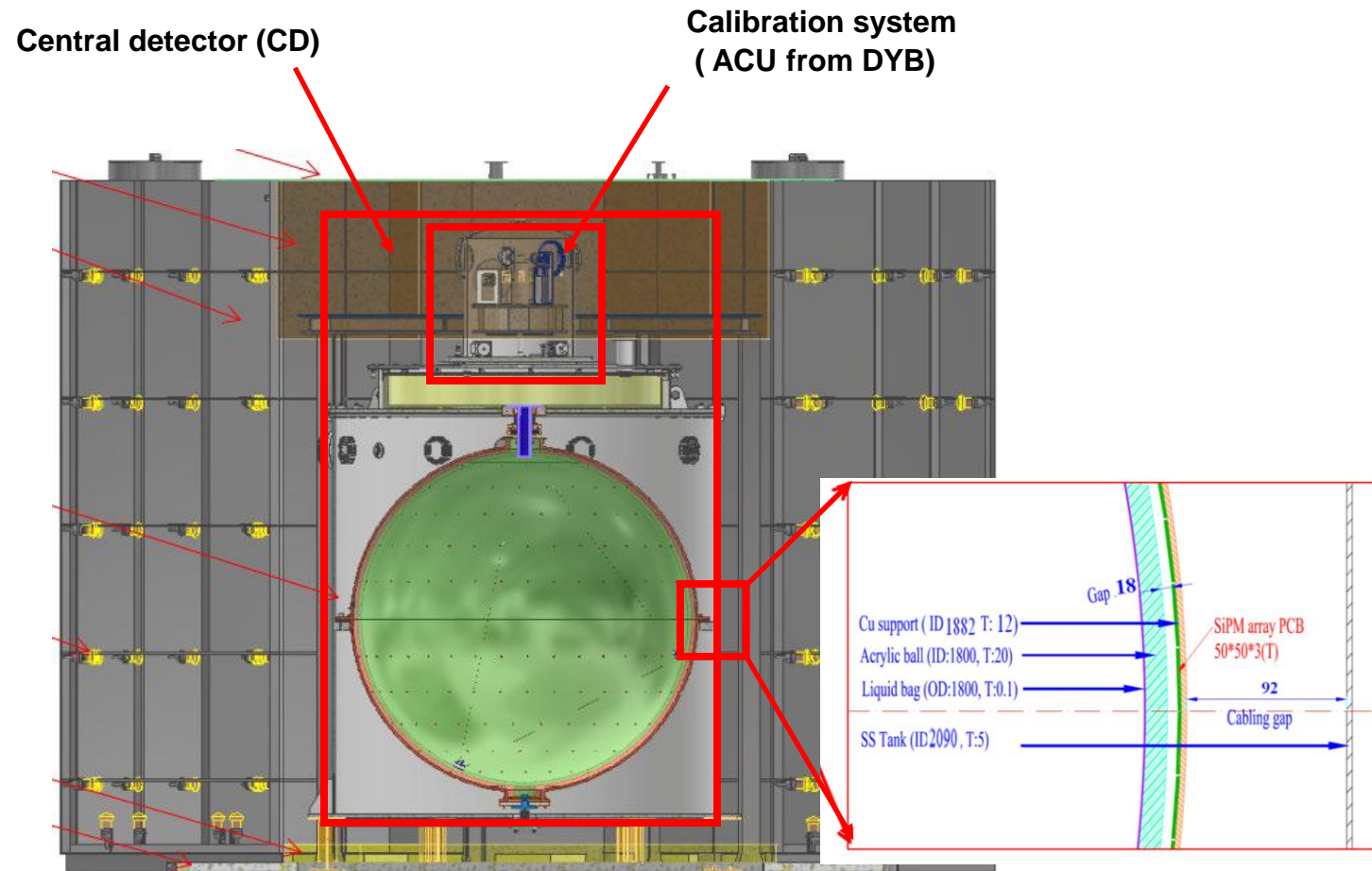


The design of the TAO detector combines the most advanced solutions in the field of LS-detectors to achieve unique characteristics. Its design uses ideas and technical solutions implemented in such experiments as DayaBay, Borexino, Juno.



TAO Central detector

- **Multilayer container**
 - Stainless steel tank (SST)
 - Copper Shell (CS)
 - Acrylic sphere (AS) vessel diameter 1.8 m
- **Cryogenic box - (- 50C°)**
 - Cooling pipes surrounding SST and CS feeding by external cooling machine
 - Melamine thermal insulation cover the SST
- **Target – LAB- based Gd-doping LS in AS**
 - Light yield 12000 photons/MeV
- **Buffer in SST - pure LAB**
- **Photosensors - 10 m² of SiPM array on the CS surface**
 - ~ 4100 50x50 mm SiPM
 - 32 SiPMs per tiles
 - photon detection efficiency > 50%
 - coverage ~ 94%
 - dark current rate < 100 [Hz/mm²]

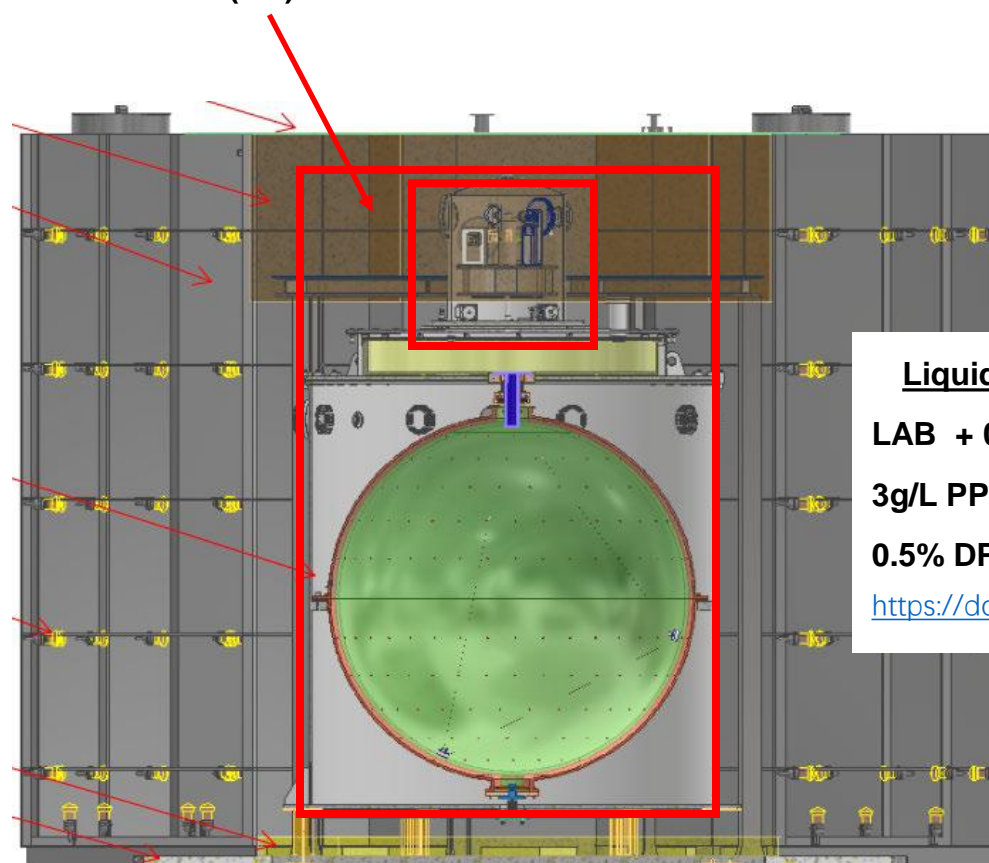


TAO Central detector

IS UNIQUE CRYOGENIC DETECTOR

- **Multilayer container**
 - Stainless steel tank (SST)
 - Copper Shell (CS)
 - Acrylic sphere (AS) vessel diameter 1.8 m
- **Cryogenic box - (- 50C°)**
 - Cooling pipes surrounding SST and CS feeding by external cooling machine
 - Melamine thermal insulation cover the SST
- **Target – LAB-based Gd-doping LS in AS**
 - Light yield 12000 photons/MeV **~25% up**
- **Buffer in SST - pure LAB**
- **Photosensors - 10 m² of SiPM array on the CS surface**
 - ~ 4100 50x50 mm SiPM
 - 32 SiPMs per tiles
 - photon detection efficiency > 50%
 - coverage ~ 94%
 - dark current rate <100 [Hz/mm²] **three orders of magnitudes down**

Central detector (CD)



Liquid scintillator recipe

LAB + 0,1% Gd

3g/L PPO + 2 mg/L bis-MSB

0.5% DPnB

<https://doi.org/10.48550/arXiv.2012.11883>

TAO Central Detector electronics



ADC FMC board

- ADC is on FEC, used to digitize analog signals from FEB
- FPGA & Power boards in MicroTCA.4 crate
- Q/T information is extracted with FPGA (waveform analysis)

Front End controller (FEC) outside the cryostat

- FMC carrier for ADC board and WR- board
- Digitize, preprocess, timestamp and pack data to send to DAQ over FO



Mini-WR FMC board



Front End Board (FEB) - inside the cryostat

- 1 tile → 2 channels
- Total 8048 channels
- Tile and FEB by connectors
- Analog signals from FEB will be transferred to FEC via differential pairs

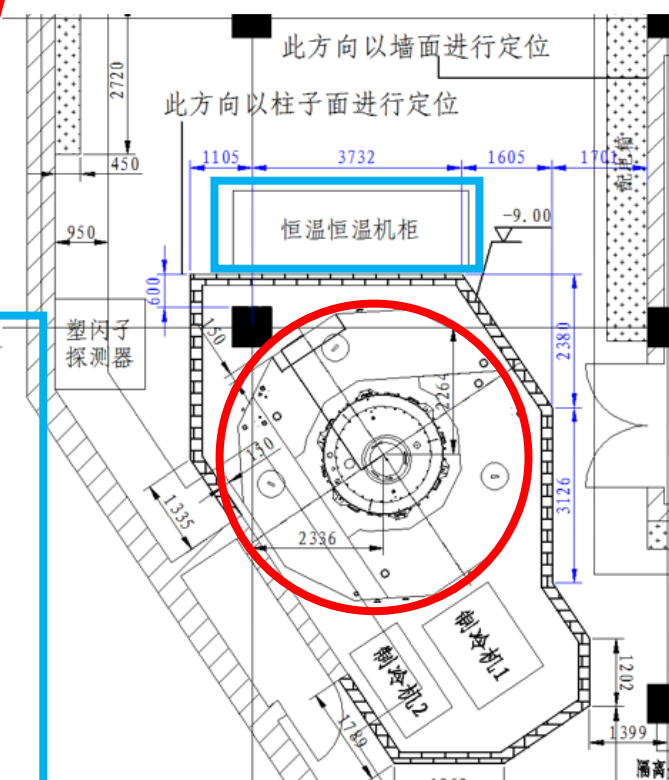
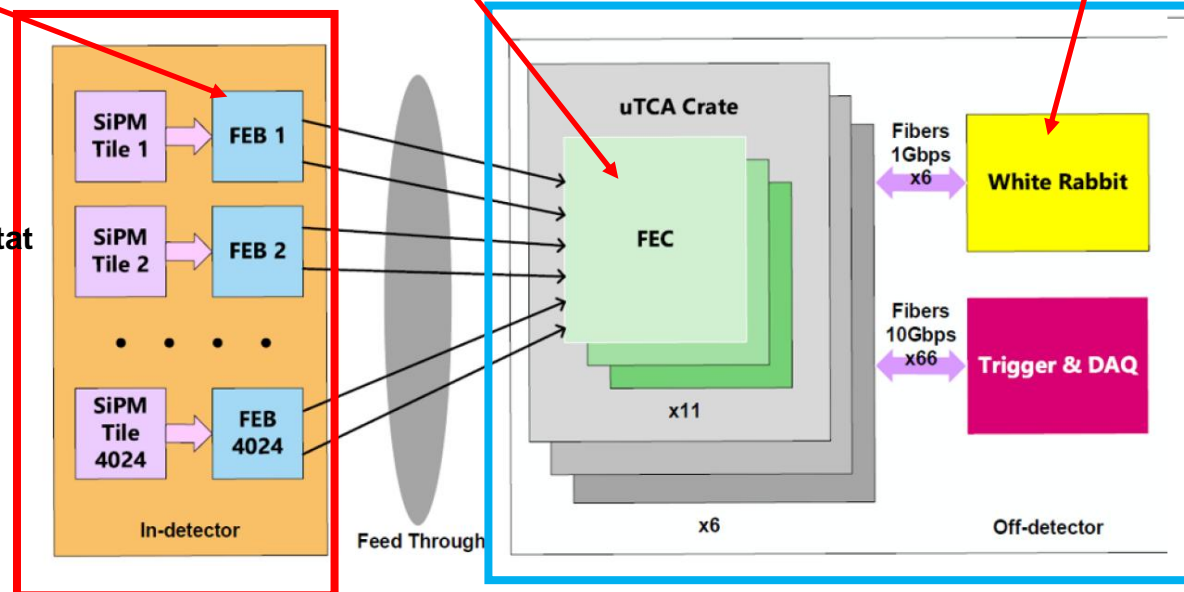
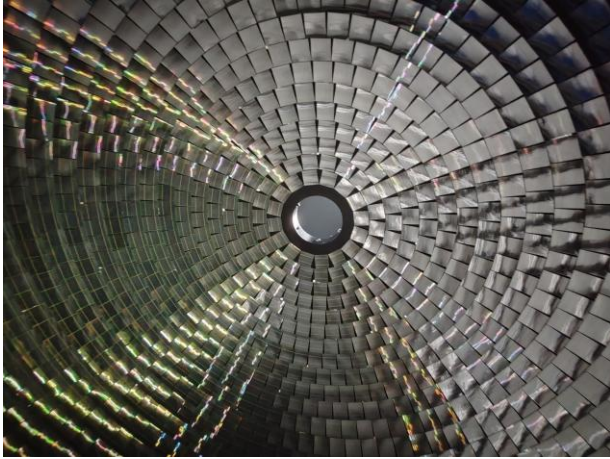


图 5.4-1 TAO 实验室消防围堰示意图

TAO Central detector commissioning at TNPP



SiPM tile commissioning

- number of tiles ~ 4100
- 50x50x3 mm 32 SiPMs per 1 tile
- photon detection efficiency > 50%
- coverage ~ 94%
- dark current rate ~100 [Hz/mm²]

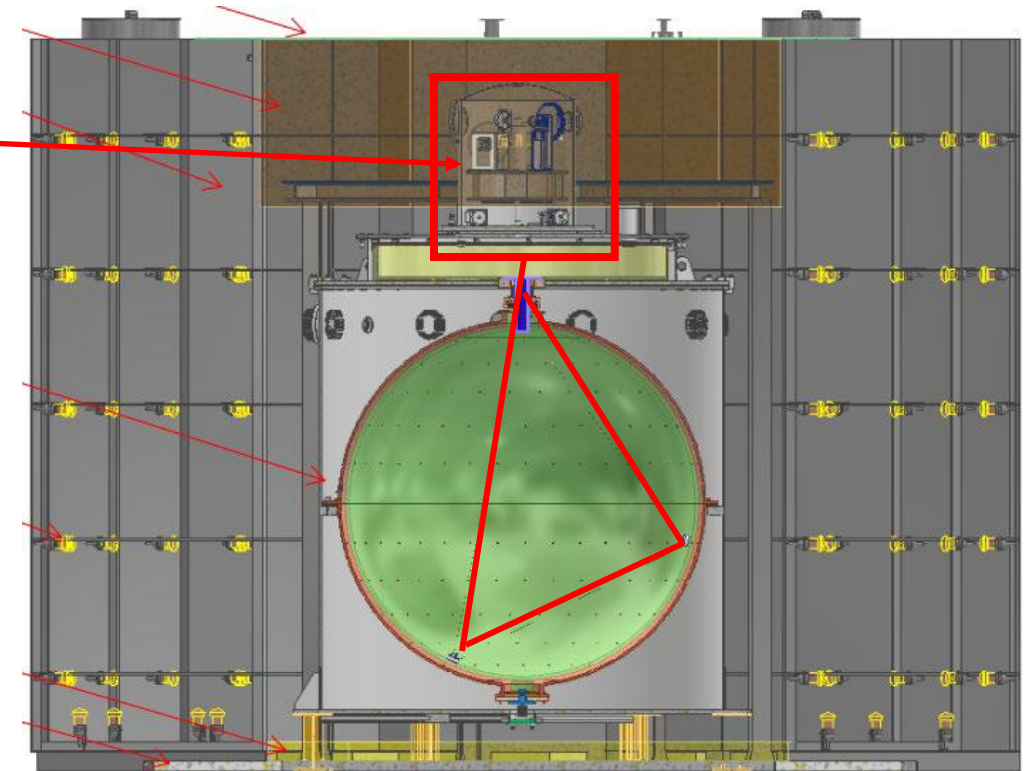
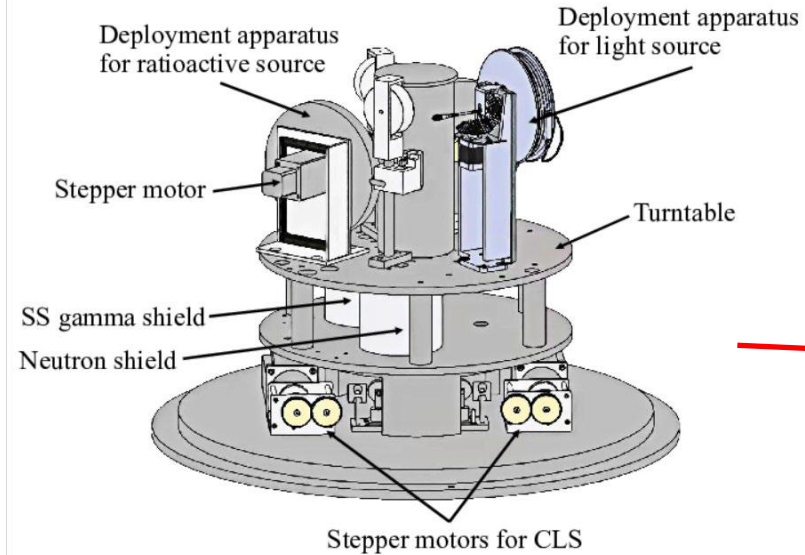
Internal cabling commissioning



TAO calibration system

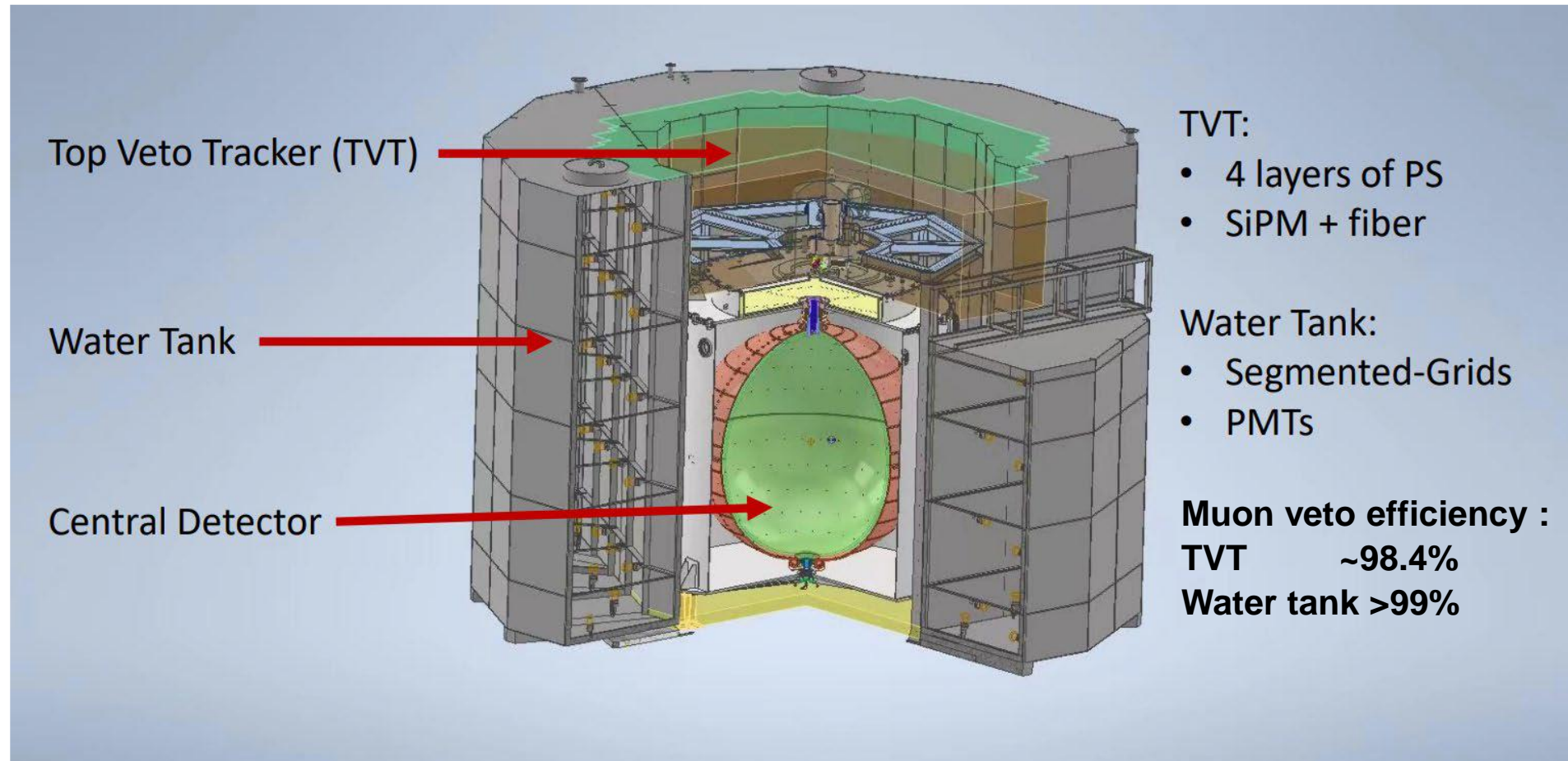
Modified from DayaBay
Automated Calibration Unit (ACU)

arXiv: 2204.03256 Calibration Strategy Paper Eur.Phys.J.C82(2022)12,1112



- **3 vertical deployment systems**
 - **gamma sources:** ^{68}Ge , combined (^{137}Cs , ^{54}Mn , ^{40}K , ^{60}Co)
 - **LED calibration system** (UV + blue)
- **cable loop system with ^{137}Cs gamma source** (SINP MSU in-kind contribution)
- **PLC-based system for remote control**

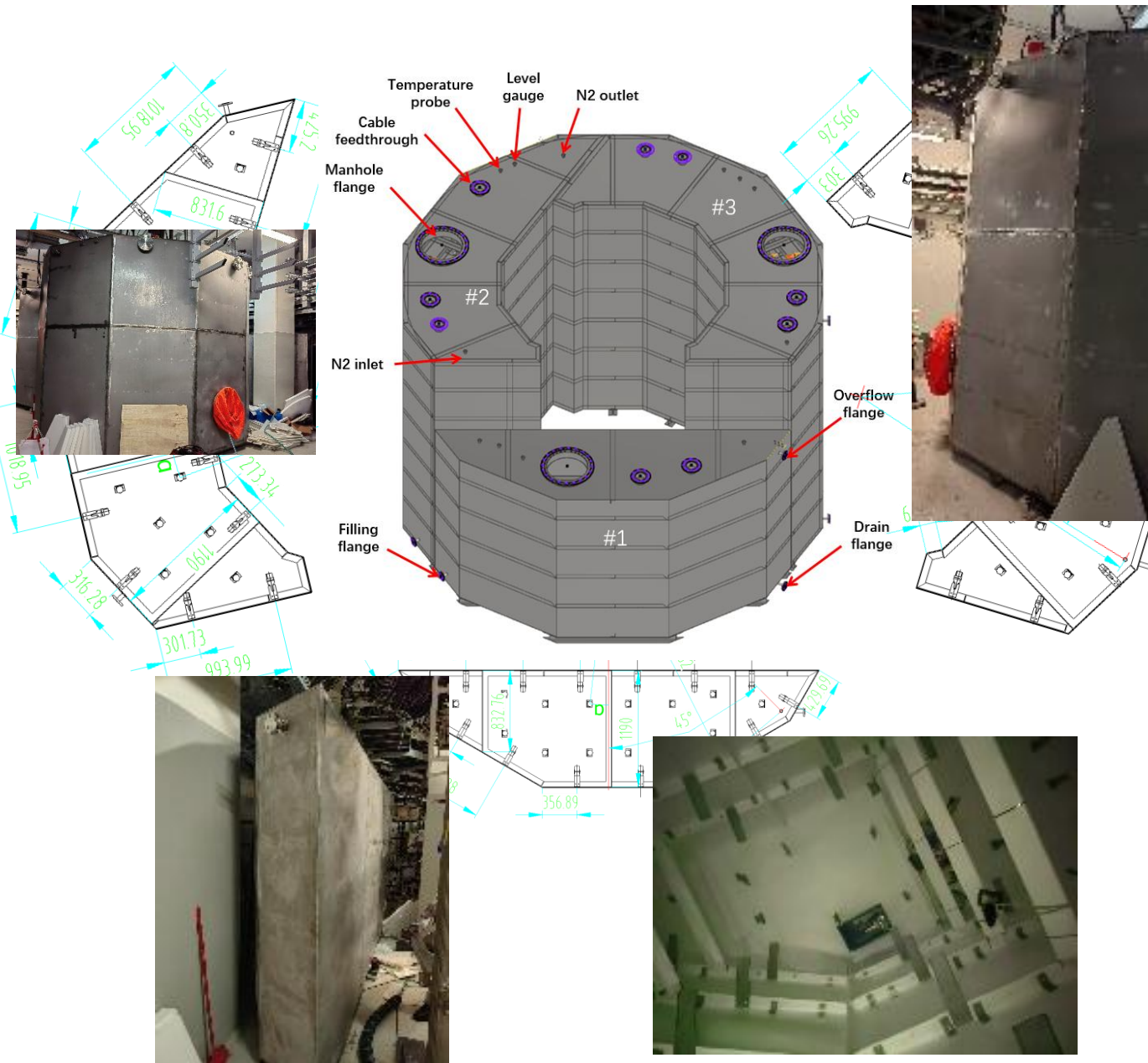
TAO background shielding and muon veto system



The expected dead time - 9.6%, according to the expected cosmic muon rate.

TAO VETO water tank (WT)

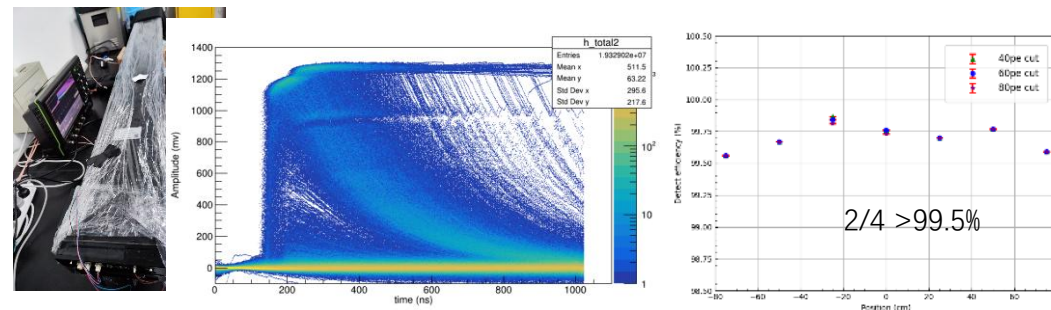
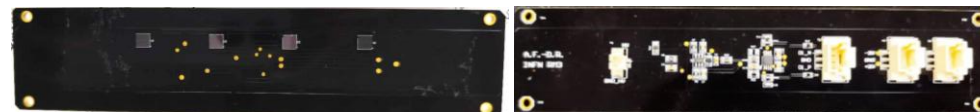
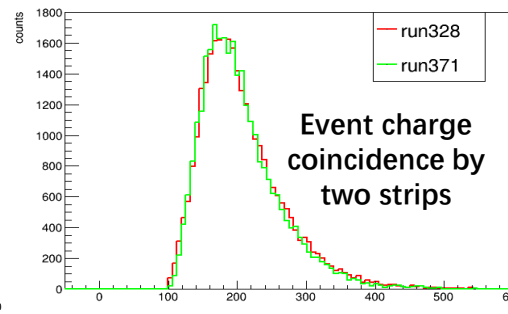
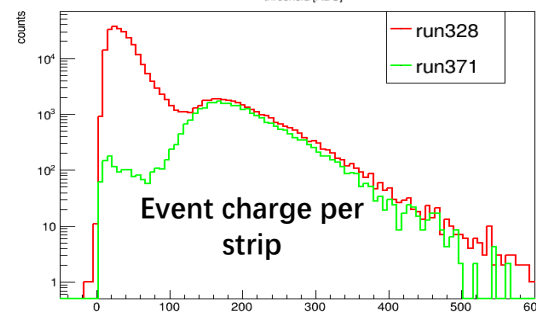
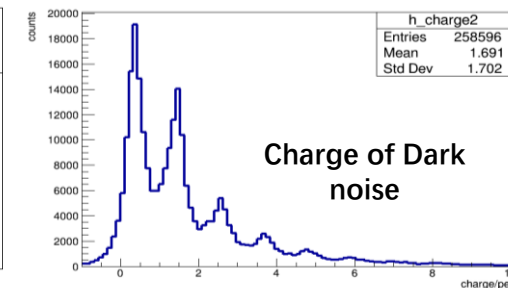
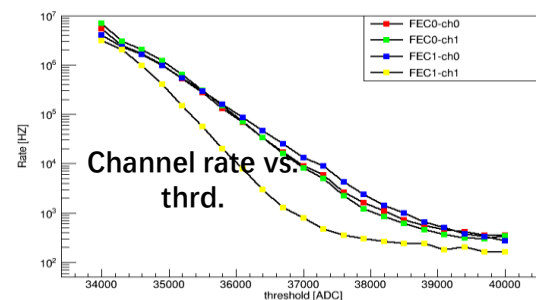
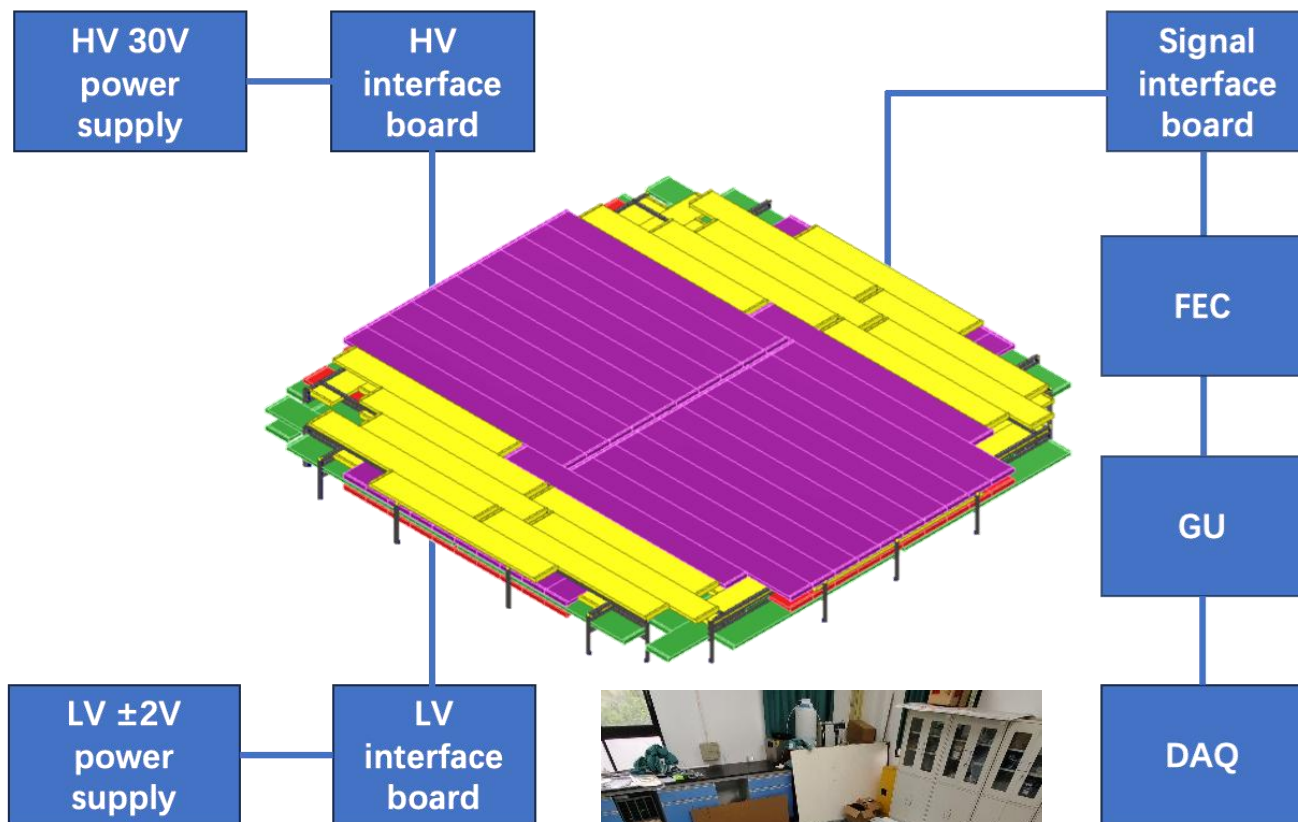
1t/h pure water system



Tyvek/PMT installed



TAO VETO top tracker (TVT)





TAO Signal and Backgrounds

The Table summarizes the signal and background rates and shape models for TAO fiducial volume

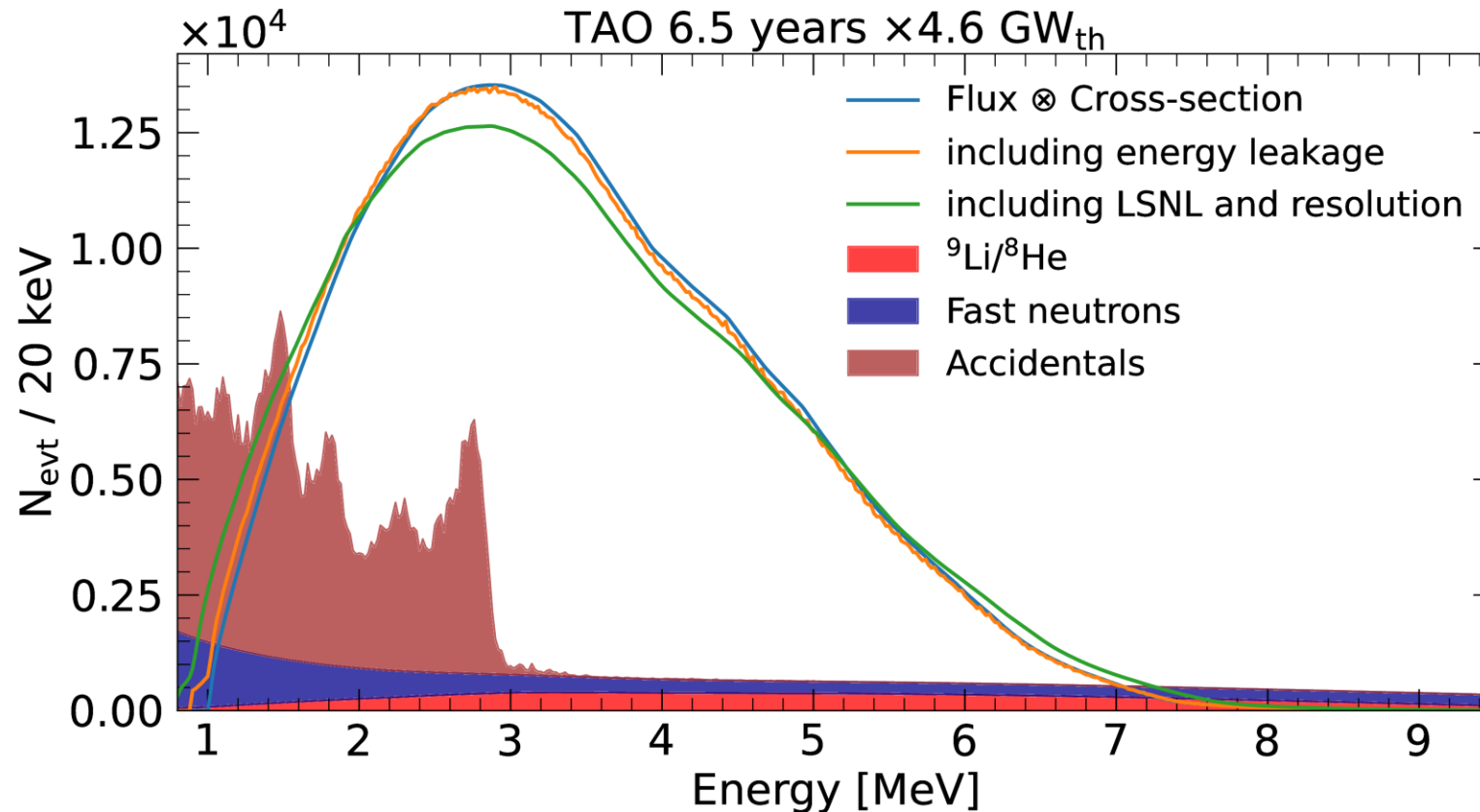
Type	Rate [day^{-1}]	Rate Uncert. [%]	Shape Model	Shape Uncert. [%]
Signal	1000	10	same as JUNO	FF, FV, ES
Fast neutron	86	–	TAO simulation	<10%
$^9\text{Li}/^8\text{He}$	54	20	same as JUNO	10%
Accidental	190	1	same as JUNO	–

FF refers to the additional fission fraction uncertainty introduced to TAO to cover the difference in burn-up history observed by TAO and JUNO

FV refers to the uncertainty due to vertex reconstruction uncertainty introduced by the fiducial volume cut

ES refers to the relative energy scale uncertainty to consider potential differences between the calibration efforts of TAO and JUNO.

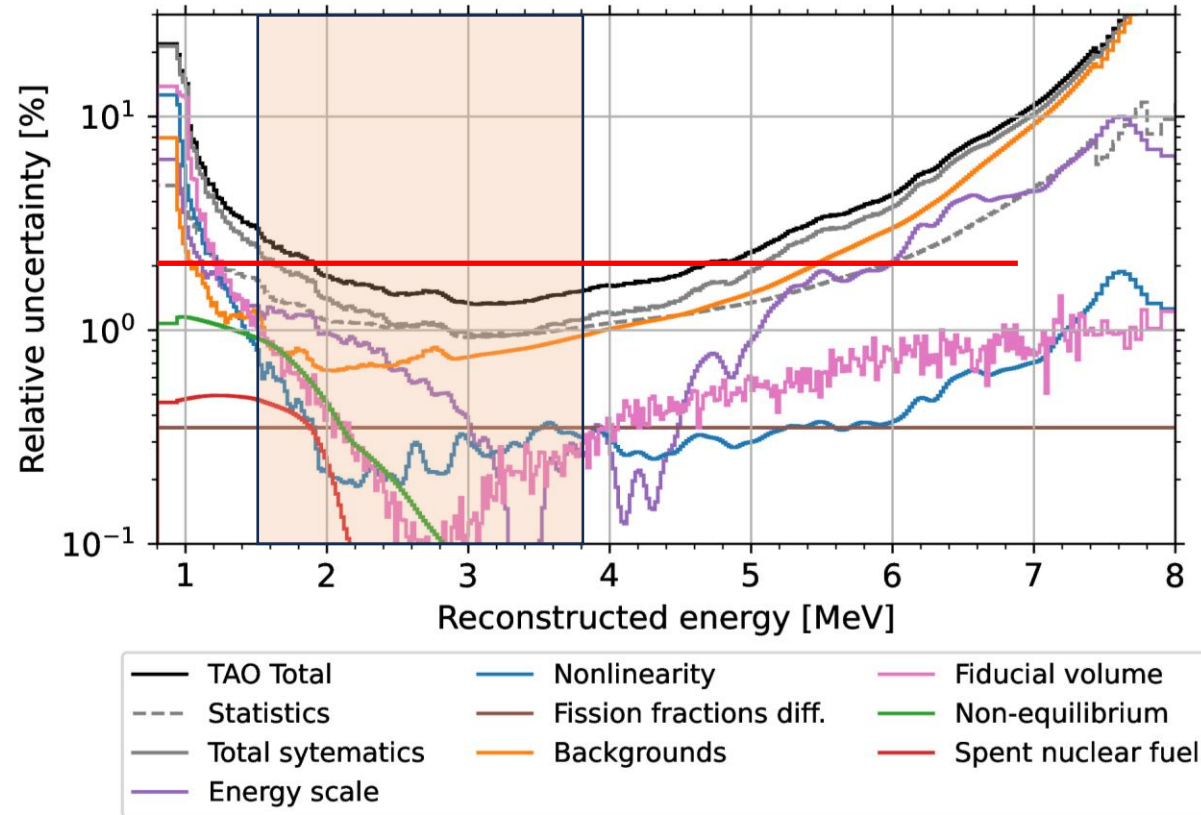
TAO Detector Response



The predicted prompt energy spectra after incorporating different effects in the energy response of the TAO detector are shown in Figure 4. The IBD positron energy spectrum is calculated with the reactor antineutrino flux from both TS-C1 and TS-C2 (4%), convoluted with the IBD cross section. Subsequently, the energy leakage effect is applied, which causes an energy shift owing to energy loss, followed by the effects of LSNL and energy resolution in sequence.

<https://arxiv.org/abs/2405.18008>

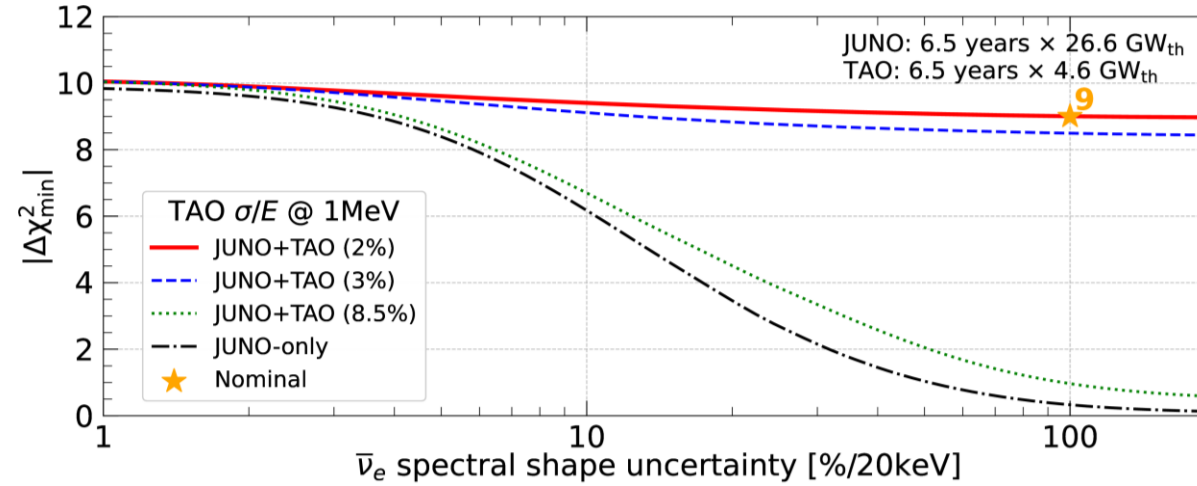
Systematic Uncertainties of the predicted spectrum to reach 3σ sensitivity to NMO



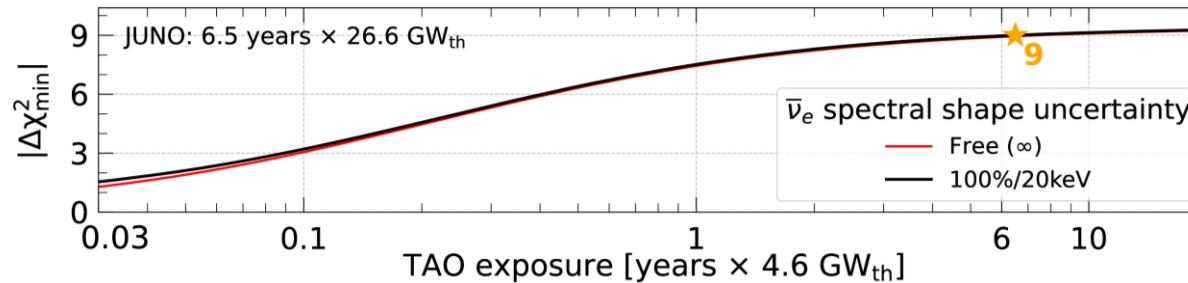
The absolute uncertainties are obtained by generating simulated samples, where systematic parameters are varied based on their assumed uncertainties and taking square roots of diagonal elements of the resulting covariance matrices.

The rate uncertainties of the spent nuclear fuel and non-equilibrium corrections, as well as of the backgrounds, also distort the observed spectrum and are consequently included in this figure. The square of the total uncertainty is a quadratic sum of all the individual uncertainties.

JUNO NMO sensitivity due to TAO energy resolution and exposure.



Nominal JUNO+TAO analysis results (marked as a star) use an exposure of 6.5 years \times 26.6 GW_{th} , nominal TAO energy resolution ($\sim 2\%$ at 1 MeV), and 100% antineutrino spectral shape uncertainty. The NMO sensitivity (red) is scanned as functions of antineutrino spectral shape uncertainty. For cases of poor energy resolution, the NMO sensitivity is also calculated by changing the TAO energy resolution to the values of Daya Bay ($\sim 8.5\%$ at 1 MeV) and JUNO ($\sim 3\%$ at 1 MeV). Without the TAO detector, the sensitivity of the JUNO-only case (black dot-dashed line) is also studied for comparison.



JUNO+TAO sensitivity versus TAO exposure time given a fixed exposure for JUNO in the cases of 100% antineutrino spectral shape uncertainty (black) and free spectral shape (red).

Conclusions (not final yet):

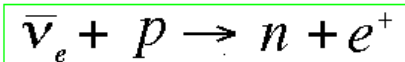
- The detector is under the final stage of installation at TNPP
- Unprecedented energy resolution of TAO-detector is expected due to symmetrical construction, low temperature scintillator and cooled photo sensors together with comprehensive active and passive shielding.
- These features open a way for precise reactor antineutrino flux and spectrum measurement which making TAO-detector a critical tool to contribute greatly to JUNO scientific program doing in parallel applied antineutrino physics

Final historical remarks:

Breakthroughs in physics in experiments with reactor antineutrinos

- 1950s (electron-anti) neutrino discovery by F. Reines and C. L. Cowan [Nobel Prize 1995]
- 1980s ROVNO, Bugey, Goesgen spectrum shape & rate reactor flux understood
- 1990s Chooz & Palo Verde — limit in θ_{13}
-corroborate Kamiokande's oscillation $\nu\mu \rightarrow \nu\tau$ dominant transition [Nobel Prize 2015]
- 2000s KamLAND / SNO favoured solar "LMA" [Nobel Prize 2015]
- 2010s Daya Bay, Double Chooz, RENO: precise spectrum, observe predicted θ_{13}

Neutrinos were first detected with a liquid-scintillation detector by F. Reines and C. L. Cowan [Nobel Prize 1995]



Detection of the Free Neutrino*

F. REINES AND C. L. COWAN, JR.

*Los Alamos Scientific Laboratory, University of California,
Los Alamos, New Mexico*

(Received July 9, 1953; revised manuscript received September 14, 1953)

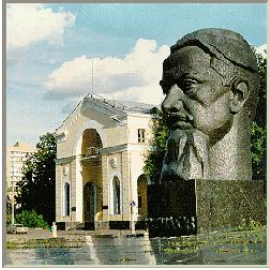
Large Liquid Scintillation Detectors*

C. L. COWAN, JR., F. REINES, F. B. HARRISON,
E. C. ANDERSON, AND F. N. HAYES

*Los Alamos Scientific Laboratory, University of California,
Los Alamos, New Mexico*

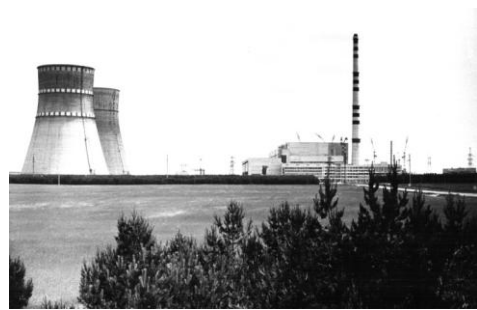
(Received February 24, 1953)

The advent of applied antineutrino physics



1974-1977

Calculation and measurement of spectra from ^{235}U & ^{239}Pu & ^{238}U & ^{241}Pu
It was shown that the number of antineutrinos per ^{239}Pu fission is less than in ^{235}U fission.
A.Borovoi, Yu.Dobrunin, V.Kopeikin. Nucl. Phys. (Rus.), 1977, 25, 264



The following ideas were expressed by L.A. Mikaelyan during the “*Neutrino-77*”:

- antineutrino event count rate enables remote monitoring of the reactor output power due to the direct relationship between $N(\text{antineutrino}) \sim N(\text{fissions})$,
- the shape of the antineutrino spectra can be a source of additional information about the isotopic composition of the reactor core

1978-1982

Several types of detectors for reactor antineutrino research have been developed (KIAE)

1982

A neutrino laboratory was created at the Rovno NPP

1983-1994

The feasibility study of the method was confirmed in experiments at the Rovno NPP (USSR) and, later, at the NPP in Bug (France) (KIAE/IN2P3).

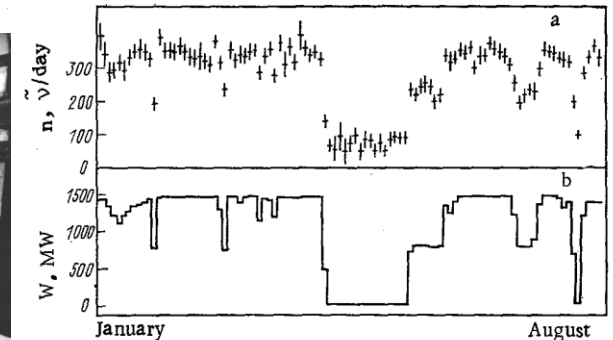
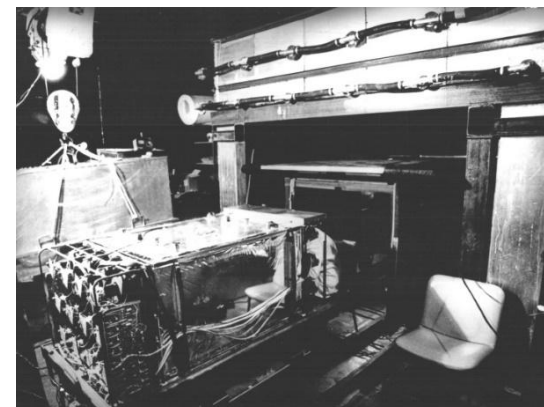
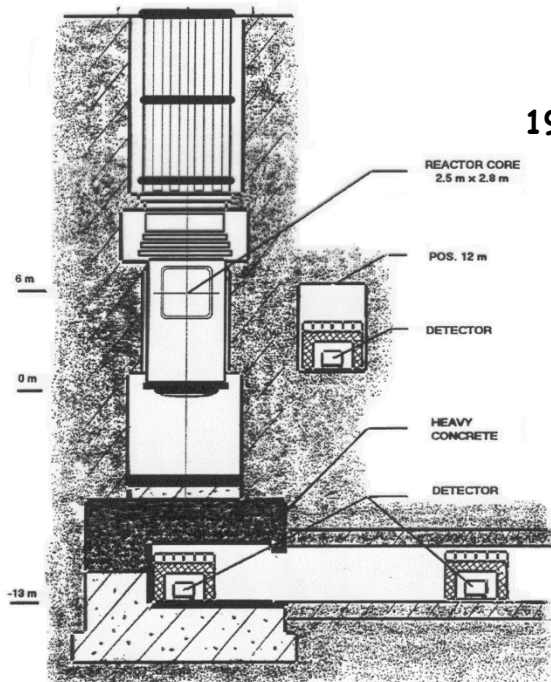


Fig. 2. Neutron instrumentation readings for January-August 1986 (a) and average daily reactor power based on data from thermal measurements (b).



Breakthroughs in physics in experiments with reactor antineutrinos

- **1950s** (electron-anti) neutrino discovery by **F. Reines and C. L. Cowan** [Nobel Prize 1995]
- **1980s** **ROVNO, Bugey, Goesgen** spectrum shape & rate reactor flux understood
- **1990s** **Chooz & Palo Verde** — limit in θ_{13}
-corroborate **Kamiokande's oscillation $\nu\mu \rightarrow \nu\tau$ dominant transition** [Nobel Prize 2015]
- **2000s** **KamLAND** favoured solar “LMA” — **SNO** complementary [Nobel Prize 2015]
- **2010s** **2010s** **Daya Bay, Double Chooz, RENO**: precise spectrum, observe **predicted θ_{13}**
- **2020s** **JUNO-TAO** will measure θ_{12} , $|\delta m^2|$, $|\Delta m^2|$ to $\leq 1\%$ **mass ordering ($\geq 5\sigma$)**

СПАСИБО ЗА ВНИМАНИЕ !